Submitted to J. Atmos. Sci.

Mesoscale Temperature Fluctuations and Polar Stratospheric Clouds

D. M. Murphy
Aeronomy Laboratory, NOAA, Boulder, CO

B. L. Gary
Jet Propulsion Laboratory, Pasadena, CA

Using both remote sensing measurements of temperature fluctuations on isentropic surfaces and in-situ measurements, we show that even high resolution trajectory calculations seriously underestimate the rate of change of temperature experienced by air parcels. Rapid temperature fluctuations will affect the activation of polar stratospheric cloud (PSC) droplets. Mesoscale temperature fluctuations are large enough to produce significant departures from equilibrium in established PSCs. Together, the enhanced cooling rates and departures from equilibrium provide a new view of denitrification and dehydration: after activation of nearly all condensation nuclei to form a PSC, mass can be redistributed to larger aerosols during the evolution of a PSC.

Introduction

Polar stratospheric clouds (PSCs) are important to stratospheric chemistry, especially the chemistry involved in polar ozone depletion. PSCS are usually grouped into two categories: Type I PSCS occur at temperatures colder than the condensation point of nitric acid trihydrate (NAT), have parts per billion of condensed material, and consist of NAT, other phases of nitric acid and water, and possibly other species. Type II PSCS occur at temperatures colder than the frost point, have parts per million of condensed material, and consist mostly of ice. This paper discusses the impact of mesoscale fluctuations on the nucleation and evolution of both Type I and Type II PSCs.

The nucleation of PSCs depends on the rate of change of temperature, as well as the temperature itself [*Toon et al.*, 1989; *Salawitch et al.*, 1989; *Drdla and Turco, 1991*]. A rapid temperature

reduction as an air parcel cools across the threshold for forming a PSC will favor nucleation on all existing p articles, while a slow temperature reduction will favor the growth of only the larger preexisting particles. Wc show here that the rate of change of temperature is seriously underestimated by trajectory calculations.]n fact, the rate of change of temperature is strongly influenced by fluctuations on scales smaller than 1O km. In contrast to the *rate* of temperature change, trajectory calculations do reproduce most of the *magnitude* of temperature fluctuations, except in mountain wave events.

The supersaturation of a condensing species responds differently 10 temperature fluctuations faster than a characteristic relaxation time than 10 slower fluctuations. Using high spatial resolution temperature measurements along With scaling laws, WC show that the small temperature fluctuations at short time scales can alter the size distribution of aerosols in established PSCs. This could enhance denitrification and dehydration if there is also a difference in the stability of some particles, such as the difference between nitric acid trihydrate and a metastable phase, Although a full microphysical model will be necessary to quantify the effects of mesoscale fluctuations on denitrification and dehydration, the brief treatment presented here demonstrates that small but rapid temperature fluctuations can alter the evolution of a PSC.

Temperature Profiler Measurements

Mesoscale temperature fluctuations in the lower stratosphere have been measured by the Microwave Temperature Profiler (MTP) aboard the NASA ER-2 aircraft. The MTP measures air temperature over an altitude region extending from approximately 2 km below to 3 km above the aircraft *[Denning et al,, 1989].* Excellent measured correlations during dives and ascents between the temperatures derived from MTP data and in situ temperatures give a very high degree of confidence that the MTP data accurately represent air temperatures above and below the airplane. The

measured temperature profiles can be converted to cross sections showing the altitude of potential temperature surfaces. If the ER-2 is flying parallel to the wind, then such cross sections represent the actual altitude and hence temperature excursions experienced by air parcels undergoing adiabatic heating and cooling. Typical wave amplitudes are 0.S K over water and 1.6 K over land at altitudes near 20 km [*Gary*, 19S9; *Bacmeister et al.,* 1990]. Figure 1 shows an example of MTP data for an ER-2 flight from California to Maine.

It is evident in examples such as Figure 1 that the heating and cooling rates are much larger in the finely resolved data than for the curve, which is smoothed to the resolution of typical trajectory calculations. For the data in Figure 1, the mean absolute value of the cooling rate is > 200 K day^{-1} for the data at full resolution, -23 K day^{-1} when smoothed to 200 km resolution, and -12 K day^{-1} when smoothed to 400 km resolution.

Power Spectra

The spectral density of measured temperatures shows the importance of small scales to the rate of change of temperature. Since mesoscale motions in the stratosphere are approximately isentropic, the desired quantity for computing temperature fluctuations is the spectra] density of temperature at constant potential temperature. Except for the limited amount of MTP data used here, we are not aware of any high resolution data sets of temperature at constant potential temperature. The Global Atmospheric Sampling Program (GASP) provided one of the most extensive sets of data for computing spectral densities [*Gage and Nastrom*, 1986; *Nastrom et al., 1986].* GASP potential temperature spectral densities were obtained along the flight paths of commercial airliners. Since airliners fly at quite constant pressure during flight legs, the measured spectra of potential temperature are approximately equal to the spectra of temperature at constant pressure, except for a scale factor $((\sim 000/p)^{.286})^2$ where p is the flight pressure in mbar.

Figure 2 shows the spectral density of temperature fluctuations versus length scale for the MTP and GASP data. Also shown on Figure 2 arc spectra of in-situ temperature measured on the ER-2 for three east-west flights [*Scott et al., 1990]*. There is agreement between the GASP and ER-2 data in spite of different flight altitudes (9 to 14 and 18 to 21 km, respectively). in general, the spectral densities Of temperature at constant pressure (as ill the GASP data) are not necessarily equal to the spectral densities at constant potential temperature (as in the MTP data). However, the spectral densities in Figure 2 arc similar for a]l.three methods, lending some confidence that GASP data can bc used to supplement the ER-2 data. The ER-2 in-situ data fall off more rapidly at high frequencies than the other data, It is not clear whether this represents a real difference corresponding to the way the data were acquired or if the difference is instrumental. A small amount of noise in the MTP and GASP data could account for the difference. Aircraft altitude "bobbing" may also affect the high frequency end of the spectrum. A more detailed treatment of the MTP-based spectral densities is underway (B. Gary, manuscript in prep.aration).

Two general properties of spectral densities arc of interest here. First, the integral of the spectral density Φ between two frequencies is equal to the contribution of those frequencies to the variance of the data. Second, the spectral density of the time derivative of a time varying signal is just $\omega^2\Phi$, where ω is the frequency [*Tolstov*, 1962]. A consequence of the derivative properly is that small scales dominate the rate of change of temperature if the slope of the spectral density of temperature fluctuations is greater than -2, whereas large scales dominate if the slope is less than -2. A variety of data shows that atmospheric spectral densities in the lower stratosphere have slopes between -1.6 and -3, with slopes commonly near -S/3 al horizontal scales of lcss than 800 kJn [*Gage and Nastrom*, 1986; *Murphy*, 1989]. Observed slopes near -2 imply that *all* spatial scales contribute significantly to the rate of change of temperature for air parcels. The abscissa of Figure 2 can bc

converted between wavenumber and angular frequency by using the wind speed.

Figure 2*b shows* the spectral density of the spatial derivative $k^2\Phi$, where k is the spatial frequency. The spectral density of the derivative shows a clear peak at synoptic scales. A wind speed u is needed to transform $k^2\Phi$, the spectrum of the spatial derivative, to $\omega^2\Phi = k^2u^2\Phi$, the spectrum of the time derivative. An average wind speed of *24 m* s^{-1} *is* used for the GASP data [*Nastrom and Gage, 1985].* Average observed winds for each flight leg, ranging from 19 to *50* m s^{-1}, are used for the ER-2 data. By integrating under the spectra in Figure 2, we obtain estimates of the mean fluctuations of the temperature and the derivative. Results are shown in Table 1. Most of the rate of change of temperature comes from wavenumbers above 0.1 km^{-1}, or wavelengths of less than 60 km.

Table 1. Temperature fluctuations by length scale

	Wavenumber Range			
	0.0004-0.01 km^{-1}	0.01-0,04 km^{-1}	0.04-0,1 km^{-1}	0,1-0.4 km^{-1}
Temp. Fluctuation	4.2 K	0.7 K	0.4 K	0.3 K
Rate of Change	19 K day^{-1}	30 K day^{-1}	51 K day^{-1}	140 K day^{-1}

Note: Contributions from more than one range should be added as the square root of the sum of squares.

Trajectory calculations using operational meteorology models will reproduce temperature fluctuations up to the highest spatial scale resolved by the model, A very high resolution (T213) model can resolve spatial frequencies $k \approx 2\pi/\lambda$ up to about 0.06 km-l [*Laprise*, 1992] and a lower resolution model with 100 km grid spacing up to $k \approx 0.03$ km^{-1}. The actual frequency limit will be less because numerical models are strongly damped near their upper frequency limits. '1'able 1 shows that although a trajectory based on an operational model can capture most of the magnitude of the temperature fluctuations, such trajectories do not reproduce the instantaneous rates of cooling

and heating shown by the observations. The observed rates of temperature change are much faster than even the fastest temperature oscillations in *Drdla and* Turn) [1991], *whose* scenarios covered oscillations with periods of 1 to 5 clays.

Cooling Rates During PSC Formation

The microphysics of aerosols sets the range of frequencies to be considered in plots like [hose in Figure 2. Two time constants are of interest for PSCs: the time to significantly change particle diameters and the time to add or significantly change the partial pressure of the condensing species. A simplified mass transfer equation is

$$dm/dt \approx 4\pi a D \beta \rho_\Delta \qquad (1)$$

where m is the mass of a single aerosol particle of radius a, D is the diffusion constant of the condensing species, $\beta = 1/(1+4\,Kn/3)$ is the transitional correction factor of the Knudsen number Kn, and $\rho_\Delta = (p_\xi - p_v)M/RT$ is the partial density caused by the difference between the partial pressure and vapor pressure of the condensing species. At PSC conditions. Equation (1) is accurate to about *20%0* compared to a full treatment of mass transfer [*Wagner*, 1982]. If ρ_Δ is approximately constant, then an aerosol particle will grow in radius by $\sqrt{2}$ or evaporate completely in a time

$$\tau_p = 2\pi a^3 \rho_p / (dm/dt) \approx a^2 \rho_p / 2D\beta\rho_\Delta \qquad (2)$$

where ρ_p is the density of the particle. Conversely, if *a* and the temperature are approximately constant, then the partial pressure will relax exponentially to the vapor pressure with a lime constant

$$\tau_g = \rho_\Delta / (N(dm/dt)) \approx 1/(4\pi a D \beta N) \qquad (3)$$

where N is the number density of aerosol particles. Qualitatively, τ_p and τ_g show that when particles are small, they grow quickly in a proportional sense but gas phase concentrations change slowly. When the departures from equilibrium ρ_Δ are large the particles grow or evaporate quickly, but the gas phase time constant is unaffected until the particles change size. If τ_p anti τ_g are comparable, then the partial pressure of the condensing species and the aerosol size change simultaneously in a more complicated manner,

We separate a discussion of τ_p and τ_g into time scales appropriate to PSCS as they start to form and once the PSCS are established. Growing aerosol particles will essentially integrate out temperature fluctuations on time scales much shorter than τ_p. Therefore, the initial size distribution of a PSC will be determined by the cooling rate over a time of order τ_p after the condensation point is reached. For a forming Type I PSC with ρ_Δ equivalent to 2,4 ppbv of HNO_3, p = 50 mbar, and a = 0,2 μm, τ_p is about 60 rein, using a diffusion coefficient for nitric acid $D \approx (0.0077/p)(T/200)^{1.75}$ $m^2 s^{-1}$ where p is in mbar. At a wind speed of 24 m s-l the maximum spatial frequency is about 0.07 km-1 and the corresponding rate of temperature change due to all larger spatial scales is greater than 50 K day-1 (Table 1). The assumed wind speed partially cancels out of this derivation: a higher wind speed implies a smaller maximum spatial frequency but a higher cooling rate for a given spatial frequency, For a spectral density Φ that varies as k^{-2} the cooling rate scales as $\sqrt{u}$.

An analogous calculation for a forming Type 11 PSC with ρ_Δ equivalent to 0.2 ppmv of 11_20 and a = 0.9 μm yields $\tau_p \approx$ 7 min. During PSC formation, τ_p and τ_g arc comparable; hence, the

supersaturation and aerosol size change simultaneously. This complicates the interpretation of the rate of temperature change over the period τ_p, but will not alter the conclusion that typical cooling rates are > 50 K day-1 over the lime it takes to establish the initial size distribution.

Supersaturation in Established PSCs

The time constants τ_p and τ_g are very different for an established PSC than they are during the initial condensation. For a Type I PSC with N = 8 cm^{-3}, and a = 0.35 μm, τ_g *is* about 23 min. For a Type 11 PSC with N = *4* cm^{-3}, and a = 2 μm, τ_g is about *80s*. In both cases, $\tau_p >> \tau_g$ so gas phase responds more quickly (ban the particles. This is due to the increased surface area in an established PSC and the reduced amount of gas phase material present after condensation. Time scales for both forming and established PSCS arc shown in Table 2.

Table 2. Sample Time Constants for Mass Transfer

Forming PSCS

	T K	N cm^{-3}	a μm	Condensed‡	s	τ_g min.	λ_g* km	τ_p min.	$\overline{\lvert dT/dt \rvert}$ K day^{-1}
Type I	194.1	8	0.2	0.6 ppbv	0.8	(2.4 ppbv)	68	86	60
Type 11	188.0	4	0.9	0.2 ppmv	0.04	(0.2 ppmv)	5	7	7
									5(I >100

Established PSCs

	T K	N cm^{-3}	a μm	Condensed‡	τ_g min	λ_g* km.	$\overline{\lvert s \rvert}$	$2\tau_p$ @ $\overline{\lvert s \rvert}$ hr
Type I	193,1	8	0.35	4.2 ppbv	23	33	0.45 (0,8 ppbv)	13
Type 1	191.0	8	0,37	5.5 ppbv	21	30	0.45 (0.2 ppbv)	64
Type II	185.4	4	2.0	2.0 ppmv	1.3	2	0.035 (o. 1 ppmv)	2

‡ Amount of condensed HNO_3 or H_20 as derived from number and radius assuming a 0,1 μm radius nonvolatile core,
* Assuming a wind speed of 24 m s^{-1}.
All calculations at 50 mbar.

Over times much larger than τ_g, the gas will have time to respond to the temperature by condensing onto or evaporating from the particles, For times less than τ_g the gas phase cannot stay in equilibrium with the particles. Wc define $\overline{|\Delta T|}_g$ as the typical temperature fluctuation over time scales too short for the gas phase to stay in equilibrium with **the** PSC particles. By integrating from the right in Figure 2*a* or Table 1 wc obtain $\overline{|\Delta T|}_g \approx 0.6$ K for the Type I PSC conditions and $\overline{|\Delta T|}_g \approx 0.2$ K for Type II PSC conditions. Temperature fluctuations with periods near τ_g contribute most heavily to the supersaturation since fluctuations over very short times are quite small.

An approximate method to estimate the mean absolute supersaturation $s = p_\xi/p_v - 1$ is to simply multiply $\overline{|\Delta T|}_g$ by the slope of supersaturation versus temperature γ. However, the spectral density

of the supersaturation can be found analytically under the assumption that the temperature fluctuations are small enough to linearize the vapor pressure $p_v \approx \gamma p_{v,o}(T-T_o)$. If the temperature dots not cross the condensation point, then the response of the supersaturation to the temperature is a linear system and will respond independently to the Fourier components of the temperature fluctuations. Under linear conditions, the response to a temperature perturbation $\Delta T(t) = A_k e^{ikx}$ is $s(t) = \gamma A_k e^{ikx}(-iku\tau_g t/(1+iku\tau_g t))$. The spectrum Of supersaturation follows as

$$\Phi_S = \gamma^2 \Phi_T k^2 u^2 \tau_g^2/(1+k^2 u^2 \tau_g^2) \qquad (4)$$

where Φ_S is the spectral density of supersaturation and Φ_T is tile spectral density of temperature. With a change of variables, Equation 4 is familiar to electrical engineers. Figure 3 shows $d(s^2)/d(\ln(k)) = k\Phi_S$ evaluated for Type I PSC conditions. By plotting $k\Phi_S$, the contributions of a frequency band to the variance s^2 is visually equal 10 the area under the **curve when** using a logarithmic scale for the independent axis. For Type I PSCs, most of the variance is duc to wavelengths of -100 km. For Type II PSCs, most of the variance is duc to wavelengths of -10 km. Equation 4 is not accurate for frequencies less than about *0,02* km^{-1} because the linearity assumption fails for large amplitude perturbations. However, these frequencies contribute little to the supersaturation.

The mean absolute value of the supersaturation can be solved analytically for the special case when $\Phi_T = bk^{-2}$ (Figure *2a),* In that case, Equation 4 may be integrated over all wavenumbers to yield

$$\overline{|s|} \approx \gamma\sqrt{b\tau_g u\pi / 2} \qquad (5)$$

where b is a scaling factor. Although the distribution is not necessarily gaussian, $\overline{|s|}$ is analogous to the standard deviation of supersaturation. For this special case, the deviation increases with the square root of the averaging time, just as in a random walk process. The values of $\overline{|s|}$ in the remainder of this paper were obtained by numerically integrating Equation 4 using the fit to Φ_T shown in Figure 2. Our fit to Φ_T uses a Slope of -5/3 between 0.0006 km^{-1} and 1 km^{-1}, a slope of -3 above 1 km^{-1}, and an added gaussian centered near 0.002 km^{-1}.

Discussion

PSC formation

Small but rapid temperature fluctuations dominate the rate of temperature change over the time scales that define the initial aerosol size distribution for both Type I and Type 11 PSCs. Typical cooling rates over the appropriate t ime scales arc ≥ 50 K clay-1. The rates of temperature change considered here, which involve cooling and heating about a slower cooling trend, arc not exactly analogous to those in most microphysical models, which usually presume monotonic cooling. An exception was the model of *Drdla and Turco [* 1991], but that model did not include temperature fluctuations with periods lcss than a fcw hours.

Such large rates of temperature change mean that there is very little discrimination bctwccn condensation nuclei (CN). *Wofsy et al. [1990]* found that cooling rates of more than about 1 K day-1 produced particles too small for substantial sedimentation. Even with some particles serving as preferential nucleation sites, the observed rates of temperature change during PSC formation arc too large for significant preferential growth of those particles. Some preliminary model calculations using preliminary MTP observations of mesoscale temperature fluctuations showed that all of the

condensation nuclei are activated in most cases (L. Poole, unpublished results, 1989). *Dye et al.* [1990] found number densities of aerosols inside a Type 1 PSC as large or larger than the CN number density outside the cloud. As a possible explanation, we suggest that rapid temperature fluctuations during cloud formation activated CN smaller than those measured by the CN instrument. Rapid temperature changes may also promote the formation of metastable phases in Type I PSCS, such as liquid solutions [*Hanson*, 1990; *Luo et* al., 1994], nitric acid dihydrate [*Worsnop*, 1993], or amorphous NAT [*Koehler et al.*, 1992].

Established PSCs

As a PSC is forming, temperature fluctuations will tend 10 cause many small particles. However, the effect of temperature fluctuations is different on an established PSC. '1'hen, temperature fluctuations can transport mass bctwccn acrosols. The transient supersaturations $\overline{|s|}$ arc surprisingly large, over 40% for Type I PSC conditions and 3.5% for Type 11 PSC conditions (Table 2). If anything, the fit to GASP data taken at -11 km underestimates the supersaturations in PSCS because some mesoscale motions, such as gravity waves, amplify with altitude.

These transient supersaturations can help resolve the difficulty pointed out by *Toon et al.* [1989]. '1'heir calculations showed that denitrification was difficult to reproduce in a microphysical model, even with dehydration. At synoptic scale cooling rates, nitric acid tends to be deposited on aerosols too small to sediment out, At that point, the nitric acid is locked into the aerosols and is unavailable for transfer 10 any icc particles that form later, even though it is thermodynamically favorable for the nitric acid 10 move to the larger and more dilute particles. *Turco et al.* [1 989] found that denitrification was possible only for a limited range of cooling rates. A later calculation by *Toon et al. [1990] showed* that an air parcel needed to spend over a week in a Type I'SC for

denitrification. Dehydration in Type II PSCs probably takes at most a few days [*Kelly et* al., 1989].

Mesoscale temperature fluctuations can change this situation, since they are very effective in producing supersaturation. These deviations from equilibrium are substantial and offer a way for nitric acid or ice to move between particles. During each cycle of warming and cooling, a small amount of each particle evaporates and recondenses. The vapor can diffuse a distance of order $\sqrt{tD}$ during the warm period. Even for $t <$ **10 minutes,** there are hundreds of particles within this distance. If some particles are thermodynamically mom stable then others, then during each temperature cycle, a little less will evaporate and a little more vapor will condense than on less stable particles. An approximate time scale for altering the aerosol size distribution is $2\tau_p$ evaluated for the conditions of the moderate supersaturations generated by mesoscale temperature fluctuations (the factor of 2 is to allow for half the time each warmer and cooler than equilibrium). In a Type I PSC at $\approx$ 193 K, transient supersaturations of 40% can alter the size distribution in less than 1 day. At 191 K, altering the size distribution takes longer, about 3 days, because there is less vapor to transfer at a given supersaturation. The corresponding time for altering aerosol size in a Type 11 PSC at 3.5% supersaturation is only hours (Table 2).

An accelerating change in size distribution can possibly take place if some of the particles are more stable than others by an amount greater than the transient changes in saturation. In that case, the more stable particles can take up vapor even as the less stable particles evaporate during a warming cycle, After many cycles, some of the less stable particles can evaporate completely to the nonvolatile cores. As particles get bigger but fewer, total aerosol surface area decreases and τ_g increases. With larger τ_g, the supersaturations produced by mesoscale temperature fluctuations may get larger and the alterations in the size distribution may accelerate.

This paper dots not address the reason *why* some particles may be more stable than others. Indeed, the Airborne Arctic Stratospheric Expedition (AASE) data show that temperature fluctuations cannot be the only factor controlling nitric acid vapor pressure. Temperature fluctuations should result in supersaturation and subsaturation with about equal frequency, but AASE observations found that supersaturations with respect to NAT were much more common than subsaturations [*Kawa et al.*, 1992]. The nitric acid vapor pressure was probably controlled by some other phase than NAT [*Hanson*, 1990; *Koehler et al.*, 1992; *Worsnop*, 1993; *Luo et al.*, 1994]. *Dye et al.* [1992] and *Larsen* [1994] proposed that the formation of NAT or a metastable phase could depend on whether some or all of the sulfuric acid condensation nuclei were frozen instead of supercooled. Mesoscale fluctuations cause temperature fluctuations so rapid that other CN may be activated even in the presence of a subset of frozen sulfuric acid nuclei. However, (hose frozen particles would provide highly favored sites for mass transfer as the PSC evolves,

There are considerable uncertainties in the estimates of transient departures from equilibrium vapor pressure, The estimates of 45% for Type I and 3,5% for Type II PSCs are based on a linear approximation, More accurate estimates could be made by imposing mesoscale temperature fluctuations on a detailed microphysical model. The observations for temperature fluctuations are also sparse in the lower stratosphere. There are only a handful ER-2 flights parallel to the wind, and the large GASP data set was collected at lower altitudes than PSCs. Finally, the characteristic temperature fluctuations used for this discussion are based on the average of the entire GASP data set, even though there are definite differences in the amplitude of temperature fluctuations above land and water [*Gary*, 1989; *Nastrom et* al., 1987]. Wind speeds are also systematically larger along the edge of the polar vortex than near the center. Besides the obvious difference that the edge of the polar vortex is warmer than the center, the difference in wine] speed could cause a systematic difference in the microphysics of stratospheric dehydration and denitrification between the edge and center of the polar vortex. The one flight showing as an outlier in Figure 3*b* did not have especially

large temperature fluctuations. Instead, it was a flight along the edge of the vortex (Feb. 20, 1989) that encountered 50 ms $^{-1}$ winds.

01(1.side the Stratosphere

Dehydration at the tropical tropopause will have time constants similar to the PSC Type I case shown here, so temperature fluctuations may be important to tropical dehydration. Because most tropospheric clouds have more condensed and gas phase mass, the time scales τ_p and τ_g are both shorter in the troposphere than in the st rat osphere. The mean supersaturat ion becomes very small but the mass transfer between aerosols is faster at a given supersaturation. These two effects roughly cancel so the time for redistribution of mass remains in the range of few hours to days for upper tropospheric clouds just as in PSCs. For example, a calculation for the high tropical clouds reported in *Knollenberg et al. [1993]* yields $\tau_g \approx 12$s and $\overline{|s|} \approx 0.7\%$. Even so, the time to transfer mass between aerosols remains well under a day. These estimates are extremely uncertain because they involve extrapolating the spectral densities in Figure 2 and the spectral densities may roll off at higher frequencies. *Politovich and Cooper [1988]* calculated the spectral density of supersaturation duc to turbulence in cumulus clouds. The mean departure from equilibrium was found to be a fcw tenths of a percent, which may be sufficient to broaden the droplet size distribution [*Paluch*, 1971]. The importance of mesoscale fluctuations in the troposphere will be limited on occasions when the supersaturations produced by other mechanisms arc larger than those from the temperature fluctuations

Jensen and Thomas [1994] found that temperature fluctuations caused by gravity waves significantly affect the albedo of noctilucent clouds. There, the effect is to suppress cloud formation because the exponential dependence of the H_2O vapor pressure versus temperature

causes more evaporation in the warm phase of a wave than condensation in the cold phase. We have investigated the magnitude of this slowing in growth for Type. I PSCs by comparing the growth rate at constant temperature to a growth rate with gaussian fluctuations. A standard deviation of 0.85 K was adopted to correspond to conditions away from mountain waves. The effect 011 the growth rate was on] y significant if average temperatures were within about 1 K oft he condensation point.

Conclusions

Mesoscale temperature fluctuations may have important effects on the microphysics of PSCs. The large rates of temperature change implied by observations suggest that most and perhaps all of the available CN will be activated when a PSC first forms. Temperature fluctuations may also affect the formation of metastable phases. Once PSCs arc formed, temperature fluctuations al different time scales have qualitatively different effect s. A L times longer than a characteristic relaxation time for the condensing vapor τ_g, condensation and evaporation can maintain supersaturations near zero and temperature fluctuations result in changes in the partial pressure of the condensing species. At scales shorter [ban τ_g, the condensing species cannot respond quickly and temperature fluctuations produce departures from equilibrium. Transient supersaturations have mean absolute values over 40% in Type I PSCs ant] about 3.5% *in* Type II PSCS. Previous models of PSC microphysics, which have only considered time scales longer than τ_g, could not have included the effects of these brief fluctuations. One of the intentions of this paper is to stimulate detailed microphysical modeling that includes the different effects of temperature fluctuations on time scales both longer and shorter than τ_g.

The conventional view for denitrification requires the activation and growth of a small fraction of

CN in order for the nitric acid to accumulate onto particles large enough to fall to lower altitudes. A variety of explanations have been offered for why some CN are preferred, but all the explanations require cooling rates slow enough for preferential activation to occur. The hypothesis presented here is that cooling rates are usually large enough for the activation of all CN, but temperature fluctuations on short time scales redistribute the aerosol mass to the most stable particles as the PSC evolves. This mass redistribution could be rapid: less than a day to a few days for Type I PSCs and less than a day for Type II PSCs. If coupled with a mechanism to explain why some particles are more stable, temperature fluctuations offer an explanation for the apparent rapidity of denitrification and dehydration which has been difficult to reproduce in models.

Acknowledgements. We thank Greg Nastrom for locating some of the GASP data used in [his paper.

A portion of the work described in this publication was carried out by the Jet Propulsion Laboratory, California Institute of Technology, under a contract with the National Aeronautics and Space Administration.

References

Bacmeister, J. T., M. R. Schoeberl, L. R. Lait, P. A Newman, and B. Gary, Srnall-scale waves encountered during AASE, *Geophys. Res. Lett.*, *17*, 349-352, 1990.

Denning, R. F., S. L.. Guidero, G. S. Parks, and B. I... Gary, instrument description of the airborne microwave temperature profiler, J. *Geophys. Res.*, *94*, 16,757-16,765, 1989.

Drdla, K., and R. P. Turco, Denitrification through PSC formation: A 1-D model incorporating temperature oscillations, J. *Atmos. Chem.*, *12*, 319-366, 1991.

Dye, J. E., B. W. Gandrud, D. Baumgardner, K. R. Chan, G. V. Ferry, M. Loewenstein, K. K. Kelly, and J. C. Wilson, Observed particle evolution in the polar stratospheric cloud of January 24, 1989, *Geophys. Res. Lett.*, *17,413-416, 1990.*

Dye, J. E., D. Baumgardner, B. W. Gandrud, S. R. Kawa, K. K. Kelly, M. Loewenstein, G. V. Ferry, K. R, Chan, and B. L.. Gary, Particle size distributions in Arctic polar stratospheric clouds, growth and freezing of sulfuric acid droplets, and implications for cloud formation, *J. Geophys. Res.*, *W*, 8015-9034, 1992.

Gage, K. S., and G. D. Nastrom, Spectrum of atmospheric vertical displacements and spectrum of conservative scalar passive additives due to quasi-horizontal atmospheric motions, J. *Geophys. Res.*, 92, 13,211-13,216, 1986.

Gary, B. L., Observational results using the microwave temperature profiler during the Airborne Antarctic Ozone Experiment, *J. Geophys. Res.*, *94*, **11,223-11,231,** 1989.

Hanson, D. R., The vapor pressures of supercooled HNO_3/H_2O solutions, *Geophys. Res. Lett.*, *17*, 421-423, 1990.

Hanson, D, R., and K. Mauersberger, Laboratory studies of the nitric acid trihydrate: Implications for the south polar stratosphere, *Geophys. Res. Lett.*, *15*, 855-858, 1988.

Jensen, E. J., and G. E. Thomas, Numerical simulations of the effects of gravity waves on noctilucent clouds, *J. Geophys. Res.*, 99, 3421-3430, 1994.

Kawa, S. R., D. W. Fahey, K. K. Kelly, J. E. Dye, D. Baumgardner, B. W. Gandrud, M. Loewenstein, F. V. Ferry, and K. R. Chan, The Arctic polar stratospheric cloud aerosol: Aircraft

measurements of reactive nitrogen, total water, and particles, *J. Geophys. Res.*, 97, 7925-7938, 1992,

Kelly, K. K., et al., Dehydration in the lower Antarctic stratosphere during later winter and early spring, 1987,1. *Geophys. Res.*, 94, 11,317-11,357, 1989.

Knollenberg, R. G., K. Kelly, and J. C. Wilson, Measurements of high number densities of ice crystals in the tops of tropical cumulonimbus, *J. Geophys. Res.*, 9S, 8639 -S664, 1993.

Kochler, B. G., A. M. Middlebrook, and M. A. Tolbert, Characterization of model polar stratospheric cloud films using Fourier transform infrared spectroscopy and temperature programmed desorption, *J. Geophys. Res.*, 97,8065-8074, 1992.

Laprise, R., The resolution of global spectral models, *Bull. Amer. Met. Soc.*, 73, 1453-1454, 1992.

Larsen, N., The impact of freezing of sulfate aerosols on the formation of polar stratospheric clouds, *Geophys. Res. Lett.*, *21*, 425-428, 1994.

Luo, B. P., S. L. Clegg, Th. Peter, R. Müller, and P. J. Crutzen, HCl volubility and liquid diffusion in aqueous sulfuric acid under stratospheric conditions, *Geophys. Res. Lett.*, *21*, 49-52, 1994.

Murphy, D. M., Time offsets and power spectra of the ER-2 data set from the 1987 Airborne Antarctic Ozone Experiment, *J. Geophys. Res.*, 94, 16,737-16,748, 1989.

Nastrom, G. D., W. H. Jasperson, and K. S. Gage, Horizontal spectra of atmospheric tracers measured during the Global Atmospheric Sampling Program, *J, Geophys. Res.*, 92, 13,201-13,209, 1986.

Nastrom, G. D., D. C. Fritts, and K. S. Gage, An investigation of terrain effects on the mesoscale spectrum of atmospheric motions, *J. Atmos. Sci.*, 44, 3087-3096, 1987.

Paluch, 1. R., A model for cloud droplet growth by condensation in an inhomogeneous medium, *J. Atmos. Sci.*, 28,629-639, 1971,

Politovich, M. K., and W. A. Cooper, Variability of the supersaturation in cumulus clouds, *J. Atmos. Sci.*, 45, 1651-1664, 19S8,

Salawitch, R. J., G. I'. Gobbi, S. C. Wofsy, and M. B. McElroy, Denitrification in the Antarctic stratosphere, *Nature, 339, 525-527, 1989,*

Scott, G. S., T. P, Bui, K. R. Chan, and S. W. Bowen, The meteorological measurement system on the NASA ER-2 aircraft, *J. Atmos. Oceanic Tech., 7,525-540,* 1990,

Tolstov, G. P., *Fourier Series,* translated by R. A. Silverman, Dover, New York, Ncw York, 1962,

Toon, 0. B., R. P Turco, J. Jordan, J. Goodman, and G. Ferry, Physical processes in polar stratospheric icc clouds, *J. Geophys. Res.*, 94, 11,359-11,380, 1989.

Turco, R. P, O. V, Toon, and P. Hamill, Heterogeneous physicochemistry of the polar ozone hole, *J. Geophys. Res.*, *94*, 16,493-16,510, 1989,

Wagner, P. E., Aerosol growth by condensation, *Aerosol Microphysics II*, *Eel,* W. 1-1. Mar-low, Springer-Verlag, Ncw York, 1982.

Wofsy, S. C., G. P. Gobbi, R. Salawitch, and M. B. McElroy, Nucleation and Growth of $HNO_3 \cdot 3H_2O$ particles in the polar stratosphere, *J. Atmos. Sci.*, *47,2004-2012, 1990.*

Worsnop, D. W., L. E. Fox, M. S. Zahnhiser, and S. C. Wofsy, Vapor pressures of solid hydrates of nitric acid: Implications for polar stratospheric clouds, *Science,* 259, 71-74, 1993,

Figure captions:

Figure 1. Temperature of the 490 K isentrope measured by the Microwave Temperature Profiler aboard the ER-2 on November 2, 1991 smoothed to a resolution of 5 km. The right hand scale shows the corresponding altitudes. The data smoothed to include only wavelengths longer than 200 km is also shown (displaced 2.5 K for clarity). Although the smoothed data preserves the magnitude of the temperature fluctuations, it dots not capture the rate of change. For these data, $\overline{|dT/dt|}$ is over 200 K day^{-1} at full resolution and 23 K day^{-1} when smoothed.

Figure 2. (*a*) Spectral density of observed temperature fluctuations for the GASP data (symbols), MTP data on the ER-2 (solid lines), and ER-2 in-situ data (dashed lines). A fit to the GASP data at low frequencies and the ER-2 in-situ data at high frequencies is also shown (thin line). (*b*) Spectral density of the spatial derivative of temperature fluctuations. MTP data are from flights 881231890221,911102, and two legs of 940204. In-situ data are from flights 881231,890220, and 890221. The fit is displaced a factor of 10 for clarity.

Figure 3. Contribution to the variance of supersaturations by wavenumber for the GASP data (symbols), MTP data on the ER-2 (solid lines), and ER-2 in-situ data (dashed lines). The plot is of $k\Phi_S$ so that the variance of the supersaturation is proportional to the visual area under the curve. These data were not taken in PSCS but rather represent the supersaturation in a PSC for representative temperature fluctuations. (*a*) Type I PSC conditions. (*b*) Type II PSC conditions.

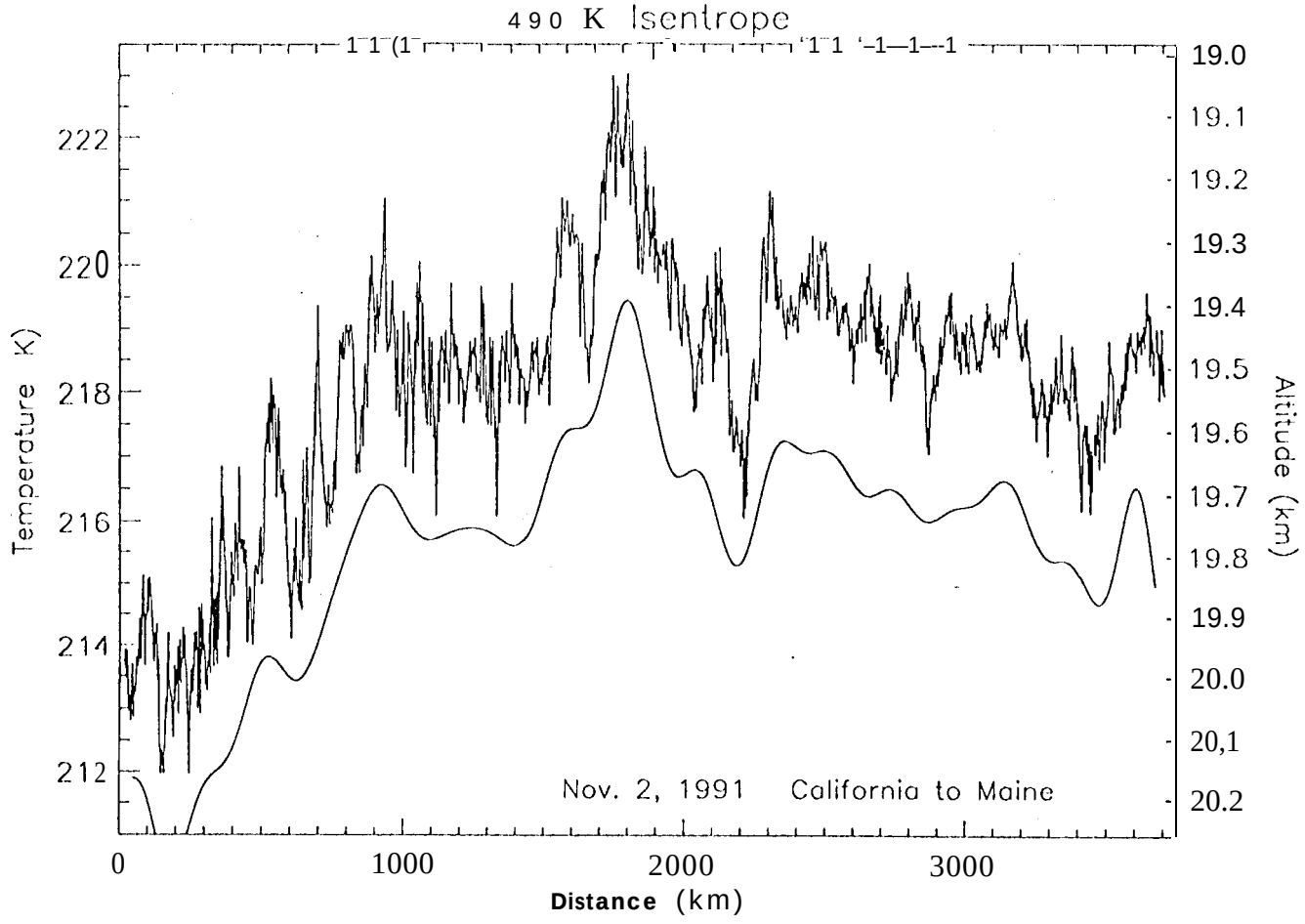

Figure 1. Temperature of the 490 K isentrope measured by the Microwave Temperature Profiler aboard the ER-2 on November 2, 1991 smoothed to a resolution of 5 km. The right hand scale shows the corresponding altitudes. The data smoothed to include only wavelengths longer than 200 km is also shown (displaced 2.5 K for clarity). Although the smoothed data preserves the magnitude of the temperature fluctuations, it dots not capture the rate of change. For these data, $|dT/dt|$ is over 200 K day^{-1} at full resolution and 23 K day^{-1} when smoothed.

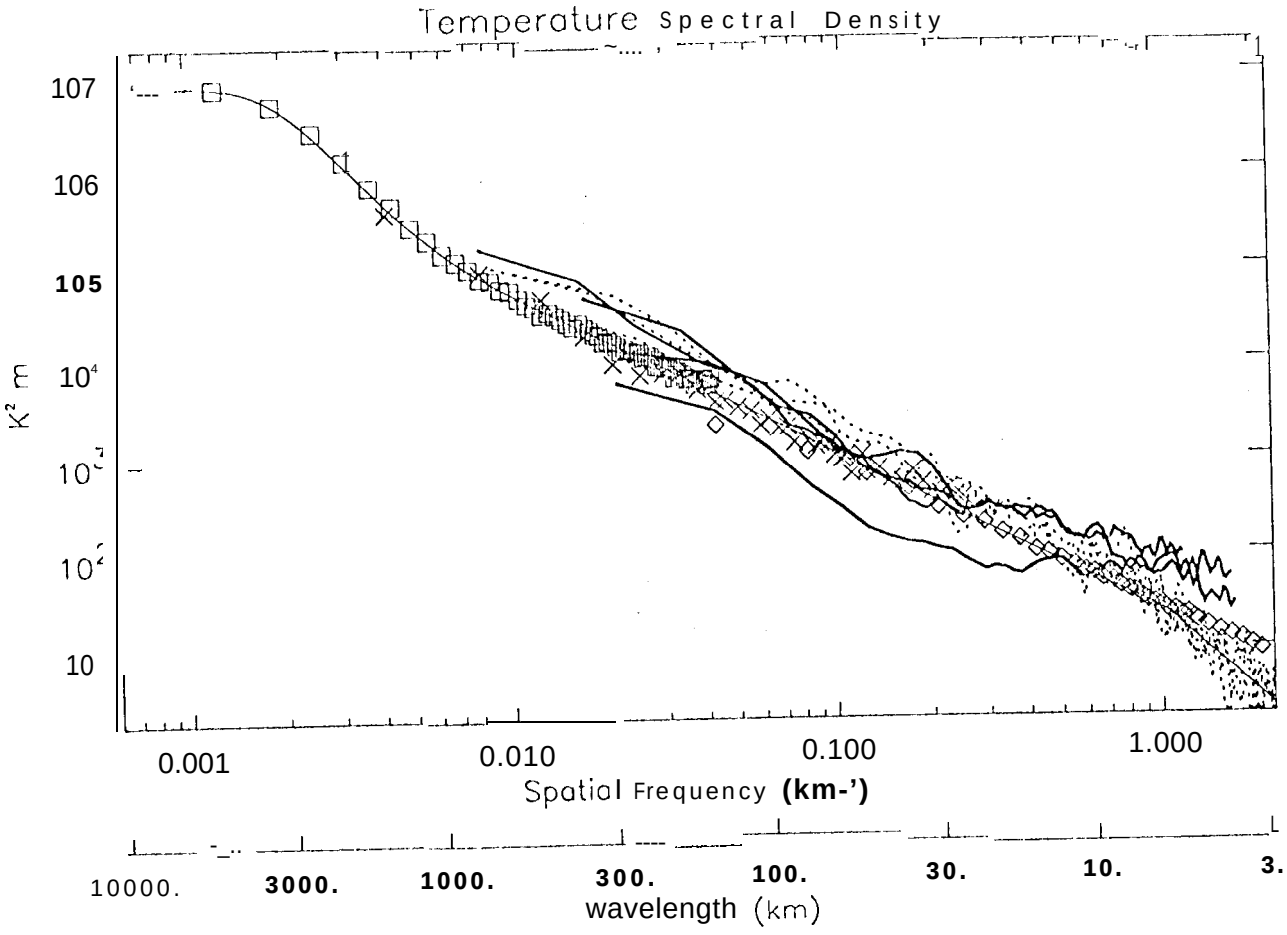

Symbols: GASP data
Heavy lines: ER-2 MTP data
Dashed lines: ER-2 in-situ data
Thin line: Fit used in calculations

Figure 2a

Fig 29

940502

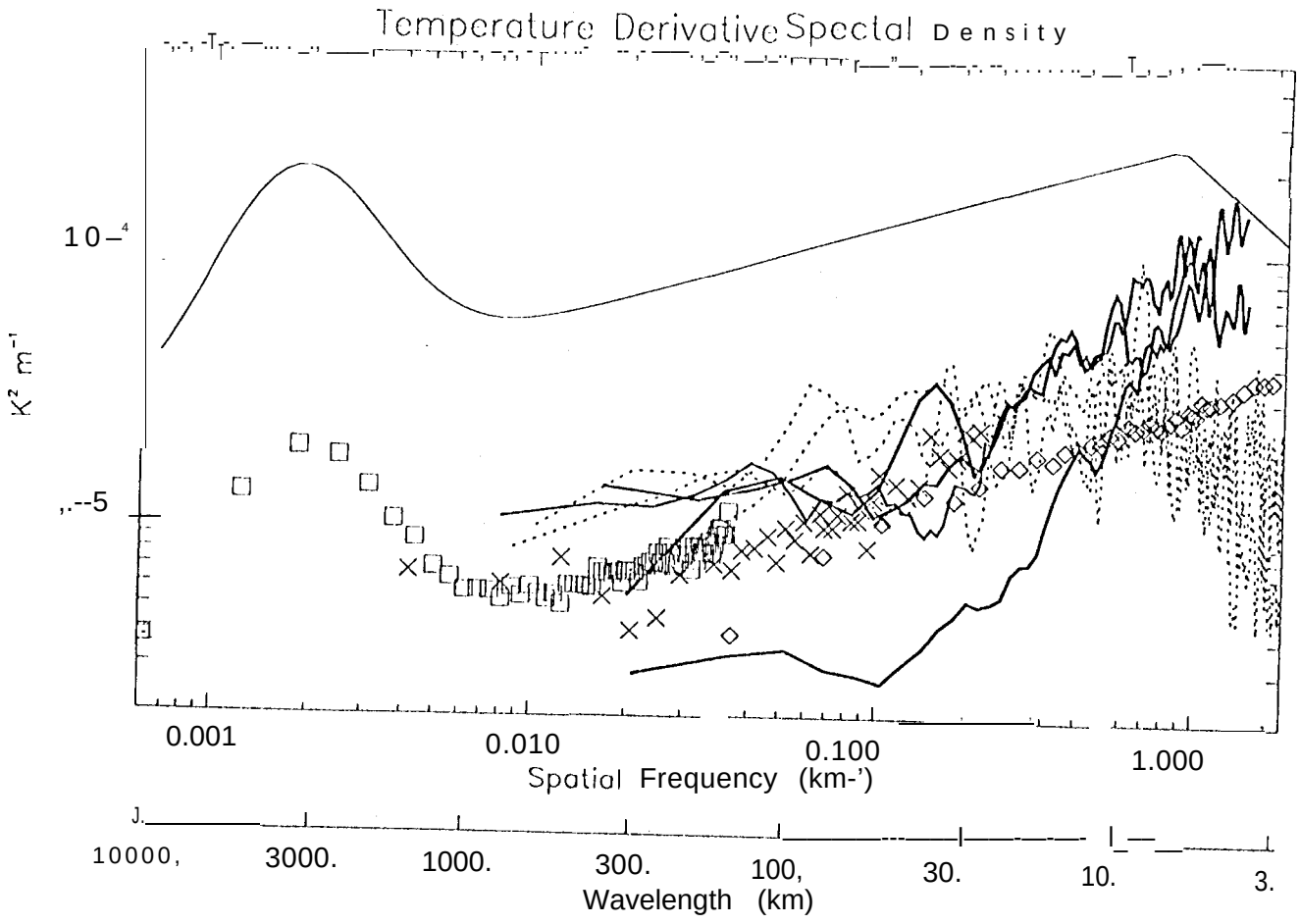

symbols: GASP data
Heavy lines: ER-2 MTP data
Dashed lines: ER-2 in-situ data
Thin line: Fit used in calculations

Figure 2*b*

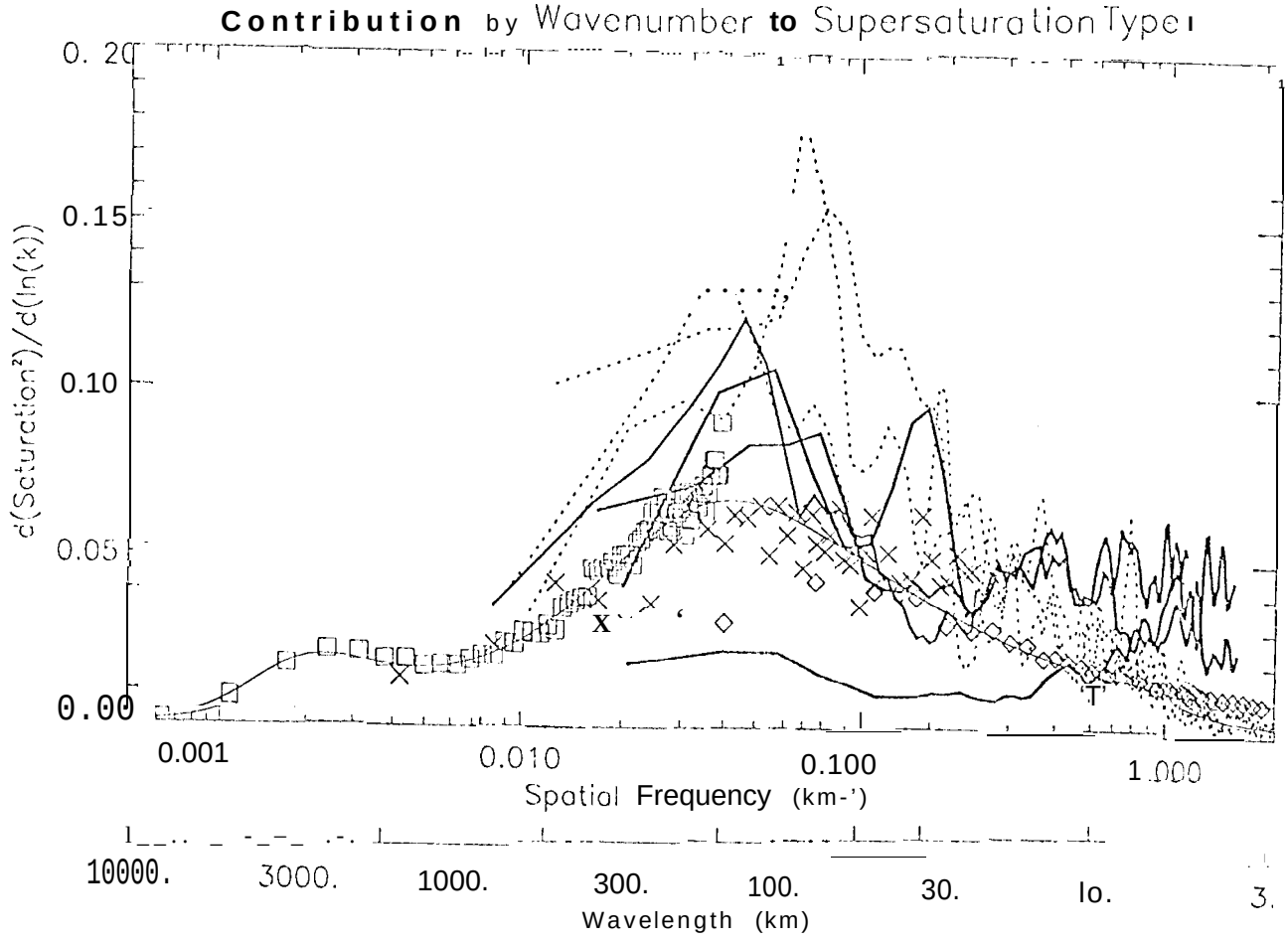

τ_g= 1300 S; γ= 0.725
Symbols: GASP data
Heavy lines: ER-2 MTP data
Dashed lines: ER-2 in-situ data
Thin line: Fit used in calculations

Figure 3*a*

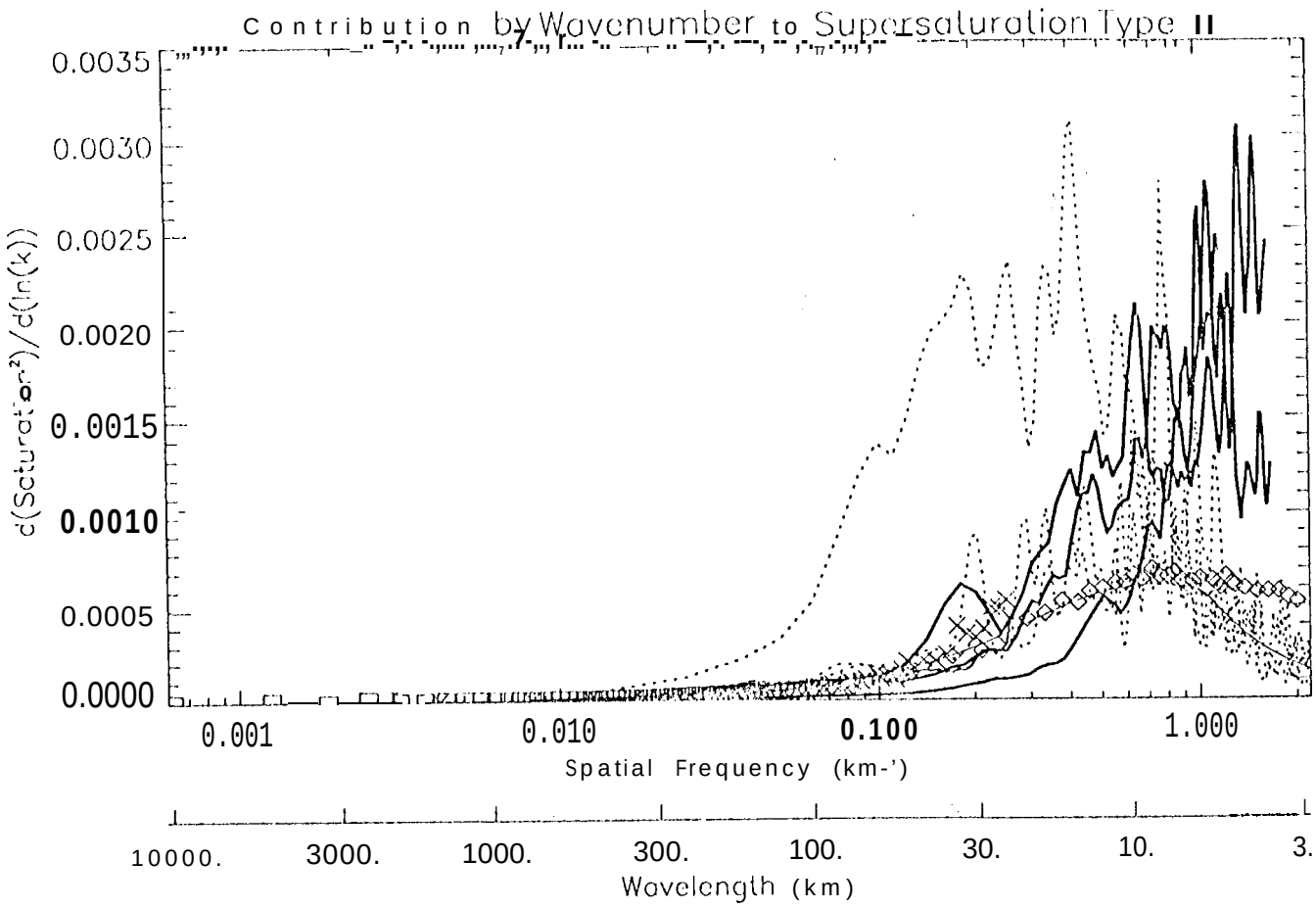

$\tau_g = 80$ s; $\gamma = 0.175$
symbols: GASP data
Heavy lines: ER-2 MTP data
Dashed lines: ER-2 in-situ data
Thin line: Fit used in calculations

Figure 3b

Fig 3b